Inducing Axial Banding in Bidisperse-by-Density Granular Systems Using Noncylindrical Tumbler Geometries

C. R. K. Windows-Yule,[1,2,3] A. J. van der Horn,[1] D. R. Tunuguntla,[1] D. J. Parker,[3] and A. R. Thornton[1]

[1]*Department of Thermal and Fluid Engineering, Multi-Scale Mechanics (MSM), MESA+, CTW, University of Twente, P.O. Box 217, 7500 AE Enschede, The Netherlands*

[2]*Institute for Multiscale Simulation, Engineering of Advanced Materials, Friedrich-Alexander Universität Erlangen-Nürnberg, Schloßplatz 4, 91054 Erlangen, Germany*

[3]*School of Physics and Astronomy, University of Birmingham, Edgbaston, Birmingham B15 2TT, United Kingdom*

(Received 13 April 2017; revised manuscript received 29 June 2017; published 17 August 2017)

We present evidence of axial banding in rotated, binary granular beds comprising particles of equal size but differing material density. It is demonstrated that the presence of differing particle densities alone may produce limited, localized axial segregation arising due to end-wall effects, but that true axial banding, i.e., axial segregation patterns pervading the full extent of the system may be induced through the use of a rotating tumbler whose internal geometry comprises alternating convex and concave segments. The segregation patterns formed are observed to be stable and reproducible, unlike the unpredictable, metastable banding typically observed in systems containing particles differing in size. Moreover, we demonstrate that, by varying the axial extent and positioning of the individual convex and concave segments, the system geometry may be deliberately tuned in order to directly control both the positions and the widths of the axial bands produced—a finding with significant potential benefits for a range of industrial processes.

DOI: 10.1103/PhysRevApplied.8.024010

I. INTRODUCTION

A. Granular segregation

The segregation [1] of granular media, whereby particles with differing geometric [2–4] or material [5,6] properties spontaneously separate, is a fascinating phenomenon crucial to numerous natural and industrial processes [7–10].

The tendency for differing "species" of particle to segregate may be exceedingly problematic in some instances, yet highly desirable—or even necessary—in others. For example, in the pharmaceutical industry, the demixing of excipient and active ingredient during the processing of medicines may carry serious, even dangerous, consequences [9]. Conversely, the presence of granular segregation is crucial to processes such as the reclamation of valuable materials from potentially hazardous waste or the separation of precious ores in the mining industry [11,12].

Whether its action is to help or hinder a given process, it is well known that a strong understanding of granular segregation is vital to the function of numerous industrial processes. However, to date, granular segregation remains—in a majority of scenarios—surprisingly poorly understood.

One example of a segregative process which is both poorly understood and of significant industrial relevance is the axial banding of granular media housed in horizontally rotating "drums" or "tumblers." The rotating-drum setup is widely used in a number of diverse industries, including the automotive, ceramics, chemical, construction, food, mining, and pharmaceutical sectors, where they perform operations such as crushing, heating, deburring, grinding, mixing, and separating. Clearly, an improved knowledge of these systems, their fundamental behaviors, and the manners in which these behaviors may be influenced and controlled is highly desirable [9].

B. Segregation in horizontally rotated drums

When housed in a horizontally rotating drum, a geometry often used in industrial settings [13,14] and relevant to numerous research fields [15], particles exhibit both radial and axial segregation. Binary systems demonstrating radial segregation typically form a "core" (see Fig. 1) predominated by one of the two species present, and an outer region comprising, largely, particles of the second species [16–18]. For adequately long drums, a system may also separate axially, producing a series of "bands," each primarily composed of a single particle type [19–22]. While both radial and axial segregation have been studied extensively, the majority of previous investigations focused on systems whose constituents differ solely in size ("*s* systems") [19–22] or in both size and density ("*s*-*d* systems") [18,23–25]. Research concerning "*d* systems," wherein particle species differ solely in their densities [26–28], meanwhile, remains comparatively limited.

Prior studies have shown that, in *s* systems, smaller particles will typically form a radial core, while *d* systems will instead produce a core of heavier particles—although density segregation is generally assumed to be somewhat

 © 2017 American Physical Society

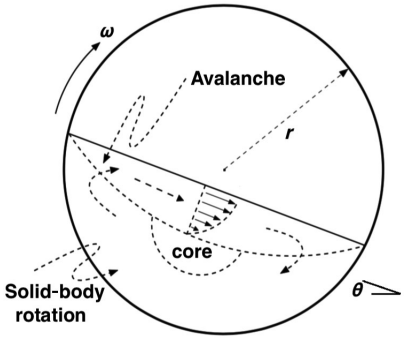

FIG. 1. Schematic diagram showing the typical delineation of the free-flowing and "bulk" regions of a rotated granular bed housed in a simple cylindrical container.

weaker than size segregation [25,29]. Recent simulation work [30,31] has indeed shown this assumption to be valid, demonstrating that the segregative behaviors of a system of particles possessing an equal size ratio and density ratio will be dominated by size effects. In such *s*-*d* systems, smaller and denser particles are found to segregate more strongly than for the equally dense case, while increasing the density of larger particles reduces segregation [18,24,25,29–31]. The similar behaviors observed for both system types suggest a parallel between the *s* and *d* systems, and hence also the density- and size-driven segregation mechanisms. Indeed, it is generally assumed that *s* systems and *d* systems can be expected to exhibit a generally similar segregative phenomenology [32,33], i.e., that qualitative observations of the former can be generalized to the latter.

However, recent studies of *d* systems provide strong, but as yet unheeded, implications that this may not be the case. Most notably, the experimental work of Sanfratello and Fukushima [26] demonstrates a distinct absence of axial banding in *d* systems despite exploring a wide range of density ratios. This absence was observed even for systems and parameter sets shown to produce strong banding in equivalent *s* systems. A similar lack of axial banding was observed in the simulations and experiments of Pereira and co-workers [25,27], with any segregation in the axial direction limited to the vicinity of the system's end walls [34]. Indeed, true axial banding in *d* systems (i.e., axial segregation pervading the entire system) has never been observed in experiment or simulation.

C. The influence of system geometry

In this paper, we observe density-driven axial banding. Specifically, we show that simply by altering the geometry of the system in which particles are housed, we are able to induce strong, clear axial bands in systems where such segregation is, under otherwise identical conditions, entirely absent.

The exploitation of system geometry as a means of influencing the segregative and/or mixing behaviors of a granular bed has previously been explored by several researchers. For example, the 2001 work of Hill *et al.* [35] studied circular and square tumblers, finding the system geometry to directly affect the observed rate of axial-band formation within a bidisperse-by-size granulate. In 2006, Meier *et al.* [36] conducted experiments using square, pentagonal, and elliptical drum geometries, showing the differing geometries to affect the form of the radial segregation patterns formed by an *s* system. This matter was later studied theoretically by Christov *et al.* [37], who focused specifically on the square and elliptical cases. In 2010, Prasad and Khakhar [38] studied the mixing of a monodisperse bed of particles, differentiated only by their coloring, in drums with various differing internal cross sections, namely, a square, a star, and a circle with either two or four triangular "wedges." It was observed that the use of noncircular cross sections acted, in some cases, to markedly increase the rate of mixing within the system. The 2015 paper of González *et al.* [39] studied the case of *s* systems with nonuniform internal geometries, specifically exploring a system comprising adjacent regions of pentagonal and pentagramal cross sections. The paper demonstrated that a bidisperse-by-size granular bed housed in such a tumbler would invariably undergo axial segregation, with smaller particles dominating the pentagramal segment of the system and larger particles the pentagonal region. The work was later extended to a range of other axially nonuniform geometric pairings [40].

Despite the appreciable volume of literature pertaining to the segregation and mixing of granular materials in noncircular tumblers there exist no prior works in which the impact of system geometry on density-driven segregation has been explored.

In this work, we utilize a series of systems similar to those originally implemented by González *et al.* [39] to provide insight into the role of system geometry in the segregation of bidisperse-by-density particle beds. Our findings provide a fascinating physical insight into the systems studied, which may potentially prove highly valuable to a variety of industrial processes where the separation of particles or powders is a necessity.

II. EXPERIMENTAL DETAILS

A. The experimental system

Our experimental system comprises a bed of N particles, composed of $N/2$ 4.0-mm-diameter glass ($\rho = 2500\ \mathrm{kg\,m^{-3}}$) and $N/2$ steel ($\rho = 7850\ \mathrm{kg\,m^{-3}}$) spheres housed in a container which is rotated horizontally about its central axis. Since all spheres possess equal diameters, the denser particles are, by definition, more massive; thus, for brevity, we denote steel particles as species h ("heavy") and glass as l ("light").

The choice of particle size and material is based on several considerations. First, as particle friction has been previously shown to induce segregation in rotated

granulates [5], we choose particles with similar frictional coefficients in order to isolate, as far as possible, the density-driven segregation mechanism in which our interest lies. For similar reasons, we also choose particles with similar restitution coefficients ($\varepsilon \sim 0.9$). The large size and (hence) the mass of particles are chosen in order to render any air effects negligible, again reducing the number of factors which may obscure the role of particle-density differences in the segregation observed. Finally, we utilize readily available materials commonly used in scientific research, meaning that our results are both comparable with prior studies and easily reproducible by other researchers.

Particles are added to the system as an initially random mixture of the h and l species. However, tests conducted in which the particles are instead sequentially added (i.e., h followed by l or l followed by h, resulting in an initially highly heterogeneous bed) are found to produce the same final steady-state distributions as equivalent, initially randomly distributed cases.

The container is constructed from a series of 9-mm axial segments, laser cut to produce various different internal geometries. The geometries of the various laser-cut segments, pictured in Fig. 2, correspond to simple, regular polygons with vertices numbering between 3 and 6, all of which are circumscribed on a circle of radius $R = 125$ mm.

By utilizing differing combinations of segments, it is possible to explore the effect of system length and internal geometry on our binary systems. In this work, our particular interest lies in the construction of systems with internal geometries which are nonuniform in the axial direction. The simple case of a system whose cross section sharply transitions from pentagonal to pentagramal at the axial center of the drum is depicted schematically in Fig. 3. However, it is also possible to construct more-complex tumbler geometries in which the internal cross section repeatedly switches between concave and convex regions.

In order to ensure consistency, the systems explored which utilize a simple, uniform, cylindrical internal geometry such as that depicted in Fig. 1 are also constructed from a series of laser-cut segments.

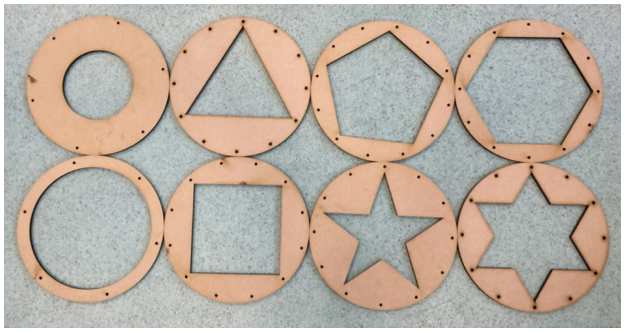

FIG. 2. Photographic image showing the different laser-cut internal geometries of the 9-mm axial segments used to form our systems.

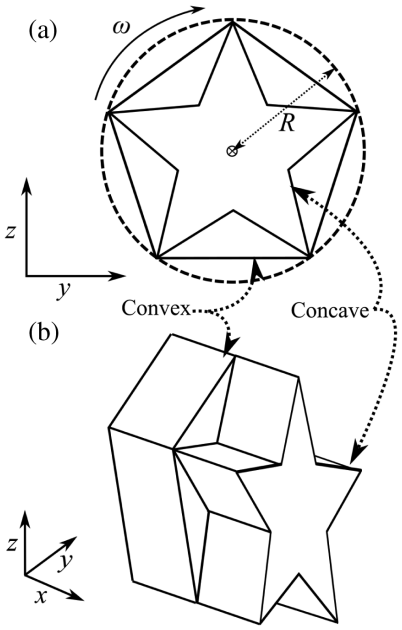

FIG. 3. Schematic diagrams representing an axially nonuniform system comprising adjacent convex (pentagonal) and concave (pentagramal) regions. The upper figure shows the system in the x-y plane, where one may more clearly see the geometries used, while the lower image provides a three-dimensional view emphasizing the axial nonuniformity of the systems employed.

In this paper, due to the time limitations inherent to the use of the positron-emission-particle-tracking (PEPT) technique, our quantitative analysis focuses primarily on a single pairing of convex-concave cross-section geometries. Specifically, we explore various combinations of pentagonal and pentagramal cross sections, as the pentagon represents the simplest convex polygon for which there exists a regular concave equivalent. Nonetheless, valuable qualitative information is also gained via visual observations of systems possessing differing combinations of internal geometry, in addition to limited additional PEPT data.

Unless otherwise specified, the drum is rotated at a constant 25 rpm ($\omega = 2.6$ rad s^{-1}), giving a Froude number $\mathrm{Fr} = [(\omega^2 R)/g] = 0.052$. As such, the system can be expected to lie within the continuously avalanching dynamic regime [41], an expectation confirmed both visually and through our experimental data.

Experiments are conducted over a period ≥ 7200 s, corresponding to a minimum of 3000 revolutions. Since axial segregation typically occurs in $O(10)$–$O(100)$ revolutions [25,32,42,43], this duration is more than adequate for our system to reach a steady, axially banded state—if such a state is indeed achievable. A majority of experiments use a filling fraction $f = \frac{1}{3}$; N is adjusted to maintain a constant f for all geometries used. The mean "concentration" or relative volume fraction, ϕ_m^h, of h particles, i.e., the fraction of the particles within the system as a whole belonging to the h species, is varied in the range $0.1 \leq \phi_m^h \leq 0.9$.

B. Data acquisition: Positron-emission particle tracking

One of the major difficulties hampering the study of axial banding in rotated granular systems is that simple, optical techniques cannot reliably image the interior of the system under investigation. The opacity of these systems to light in the visible spectrum not only makes it impossible to visualize the internal dynamics but also restricts knowledge of the segregation pattern itself, as one is typically unable to determine whether the observed bands are simply surface phenomena or if their presence extends deeper within the bed.

In order to overcome this issue, we acquire data using positron emission particle tracking, a nonintrusive technique which tracks a single, radioactively labeled tracer particle in three-dimensional space with submillimeter accuracy and millisecond-scale temporal resolution, even within the interior of deep, dense, and/or opaque systems [44].

In this work, where the bed to be explored is bidisperse, we utilize both glass and steel tracers. Glass tracers are irradiated using a helium-3 beam produced by the University of Birmingham's in-house cyclotron. When exposed to the beam, oxygen atoms within the glass (SiO_2) particles are converted to the β^+-emitting radioisotope ^{18}F via the reactions

$$^{16}O(^{3}He, p)^{18}F \tag{1}$$

and

$$^{16}O(^{3}He, n)^{18}Ne \rightarrow {}^{18}F. \tag{2}$$

For the steel particles, iron atoms are converted to ^{55}Co, also a positron emitter, via exposure to a high-energy proton beam:

$$^{56}Fe(p, 2n)^{55}Co. \tag{3}$$

The β^+ ions emitted by our activated particles will annihilate rapidly with electrons within the dense media of the tracers used, producing pairs of γ rays whose trajectories are separated by $180 \pm 0.5°$. Since the γ photons are emitted effectively "back to back," if both members of a γ-ray pair interact with the opposing faces of the dual-headed positron camera utilized in our experiments, it is possible to algorithmically reconstruct the path followed by the photons. Thus, for an adequately large number of detections, it is possible to determine the intersection point of multiple such reconstructed paths, and thus to determine the position of our tracer. Owing to the high activities utilized in our experiments, particle locations may be calculated in rapid succession, allowing the motion of the tracer particle to be accurately recorded.

The activated tracers utilized are physically identical to others of the same species within our system, meaning that for ergodic, steady-state systems such as those explored here, the time-averaged motion of a single tracer may be used to extract a variety of one-, two-, and three-dimensional fields corresponding to the behavior of the system as a whole [45]. The PEPT technique has been successfully applied to a wide range of systems, both dilute and dense, including numerous studies involving rotating-drum systems such as those explored here [39,40,46–49]. Comparison with other experimental and computational methods [39,50,51] has clearly shown the ability of PEPT to accurately capture the dynamics and segregative behaviors of these systems.

Below, we describe in detail the manners in which the fields most relevant to the current study may be extracted from PEPT data.

1. Determining particle-density fields

Consider a horizontally rotated, monodisperse granular bed which contains a single tracer particle, identical to all others in the bed. If the system is allowed to reach and maintain a dynamic steady state for an adequately long period of time, the tracer can be expected to have explored the entire system.

If we subdivide the experimental volume into a series of equally sized three-dimensional "cells," we can measure the time spent by the tracer within each of these individual cells and, from there, determine the local "residence fraction", F_R, i.e., the fraction of time spent by the tracer within a given cell.

For an ergodic, steady-state system, the particle density corresponding to any given cell is directly proportional to the residence fraction, meaning that the local particle (number) density within the ith cell of the system can be simply determined as

$$n(i) = \frac{NF_R(i)}{V_c}, \tag{4}$$

where N is the total number of particles in the system as a whole and V_c is the volume of a cell.

With a known three-dimensional distribution of particle densities within the system, it is now trivial to compute one- or two-dimensional particle-density distributions simply by depth averaging through the relevant dimension(s).

2. Determining species concentration distributions

For systems containing N_{species} distinct species of particle, it is possible to determine a particle-density distribution, as described in Sec. II B 1, for each species individually by conducting N_{species} identical repeat experiments, each using a different tracer.

In the current case of $N_{\text{species}} = 2$, we therefore conduct two identical runs for each data set, one utilizing a glass tracer and the other steel, producing two distinct particle-density fields. With this information at hand, the relative volume fraction or concentration, ϕ, of a given species at

any given point in the system (i.e., in the ith cell) can be determined as

$$\phi_h(i) = \frac{n_h(i)}{n_h(i) + n_l(i)}, \qquad \phi_l(i) = \frac{n_l(i)}{n_h(i) + n_l(i)}, \tag{5}$$

where the subscripts h and l denote, respectively, heavy and light particle species. By performing this calculation for all cells in the system and appropriately depth averaging the data produced, two-dimensional concentration distributions such as those depicted in Fig. 6 may be produced.

With a known particle concentration distribution, it is also possible to provide a simple scalar value, the segregation intensity (I_s) through which one may quantify the degree of segregation exhibited by a system. The segregation intensity is defined as

$$I_s = \frac{1}{I_s^{\max}} \left(\sum_{i=1}^{N_c} \frac{(\phi_j^i - \phi_j^m)^2}{N_c} \right)^{1/2}. \tag{6}$$

In the above equation, N_c gives the number of cells into which the experimental volume is subdivided, with ϕ_j^i representing the concentration of species j in the ith cell of the system, and ϕ_j^m the mean concentration of particles of species j in the system as a whole. The value is normalized by a quantity $I_{\max}$ which corresponds to the maximal achievable value of the term $\{\sum_{i=1}^{N_c}[(\phi_j^i - \phi_j^m)^2/N_c]^{1/2}\}$ such that I_s lies between a value of 0 (perfect mixing) and unity (complete segregation).

For further information regarding the PEPT technique and its application to bidisperse systems, please refer to Refs. [44,45,52–55].

III. RESULTS AND ANALYSIS

For simple, cylindrical drum geometries, axial banding is found to be absent across the entire parameter range explored, as expected from prior studies. For all particle concentrations $[\phi_m^{h,l} \in (0.1, 0.9)]$ and drum lengths $[L \in (90, 270)$ mm], the distributions of l and h particles exhibit only the end-wall-induced segregation expected from previous works [25,27], with no evidence of "true" axial banding—i.e., no significant concentration variations within the main body of the system. The broad general form of the particle distributions is shown in Fig. 4. The lack of axial banding across a wide range of system sizes is further illustrated in Fig. 5—for all cylindrical systems [the images in Figs. 5(a)–5(c) and 5(e)], we see a distinct lack of modulation in the radius of the h-particle core formed, indicative of an absence of axial banding.

When the cylindrical geometry is replaced with an alternating arrangement of (convex) pentagonal and (concave) pentagramal segments, however, we see strong, clearly defined axial banding. Examples of this banding may be seen in Fig. 6, while Fig. 5(d) directly shows the

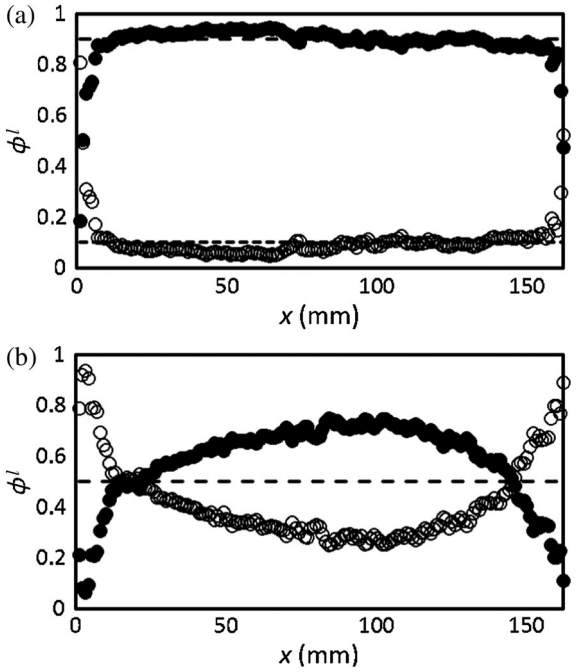

FIG. 4. Variation with axial position, x, of the local concentration of heavy and light particles, $\phi^{h,l}$. Data are shown for systems possessing mean concentrations, ϕ_m^h, equal to (a) 0.9 and (b) 0.5. In each image, ϕ^h is represented by filled circles and ϕ^l by open circles, with dashed and dotted lines, respectively, representing ϕ_m^h and ϕ_m^l.

narrowing and broadening of the h-particle core, similar to the observations of Hill and co-workers [21,42,56] for bidisperse-by-size (s) systems—though, as discussed shortly, driven by differing mechanisms.

As noted by prior researchers exploring axial segregation in bidisperse-by-size systems [21], a radially segregated core of particles remains even in the "banded" state, as may be seen in Figs. 5 and 6. While the core persists throughout the majority of the system's axial length, its diameter fluctuates considerably, breaching the surface to form dense-particle bands at some axial positions and becoming almost vanishingly small at others, being only $O(1)$ particle diameter in width. As such, the system is not fully segregated along its entire length. This behavior once again forms a direct analog to the behaviors of the smaller particle species of axially banded s systems [21].

Systems formed with relatively small concave and convex segment lengths $dx < 36$ mm, irrespective of the total drum length, possess relatively consistent global segregation strengths lying in the range $0.4 \lesssim I_s \lesssim 0.5$. However, on a local level, the axial centers of the individual h-particle bands are observed to achieve purities approaching 90%. As noted briefly above, the discrepancy between local band purity and global segregation strength is unsurprising, as the undulatory nature of the h-particle core will provide a continuous, as opposed to a sharp, transition between h-species bands and l-species bands. By

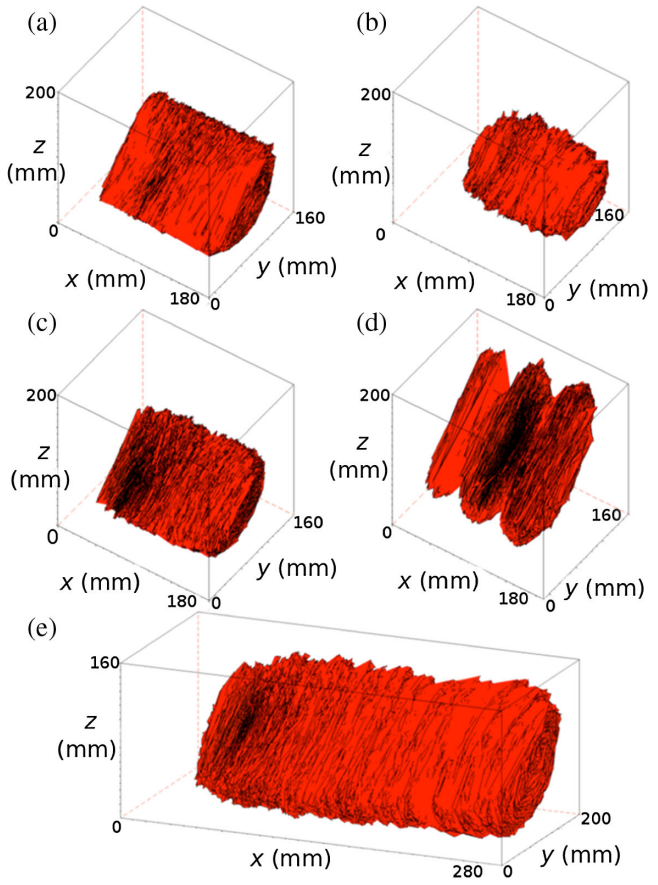

FIG. 5. Three-dimensional visualization of the radial cores of h particles formed for various systems. (a)–(c) Uniform cylinders with $L = 162$ mm and mean concentrations $\phi_m^h = 0.8$, 0.2, and 0.5, respectively. (d) A system with $L = 162$ mm whose internal geometry alternates between convex and concave along the axial direction, with six alternating pentagonal and pentagramal sections, each 27 mm wide. (e) A uniform cylinder with $L = 270$ mm and $\phi_m^h = 0.5$. For all images, $f = 0.33$.

definition, the continuous nature of this transition will create a finite number of regions in which both species coexist in comparable numbers, thus lowering the overall I_s value when averaging over the system as a whole.

It is important to note that the induced axial segregation is not limited to the specific pentagon-pentagram combination discussed above. Simple, visual observations of other convex-concave pairings clearly show the presence of axial banding for various convex-concave permutations of the polygonal cross sections listed in Sec. II A.

For all convex-concave drum geometries explored, irrespective of the system length or the ordering of convex and concave regions, the heavier species is observed to predominate convex regions, and the lighter species concave regions. This is the first time such segregation has been demonstrated for bidisperse-by-density systems.

Because of the reliance of PEPT analysis on the time averaging of the data, it is impossible to precisely quantify the rate of segregation within the system. However, by

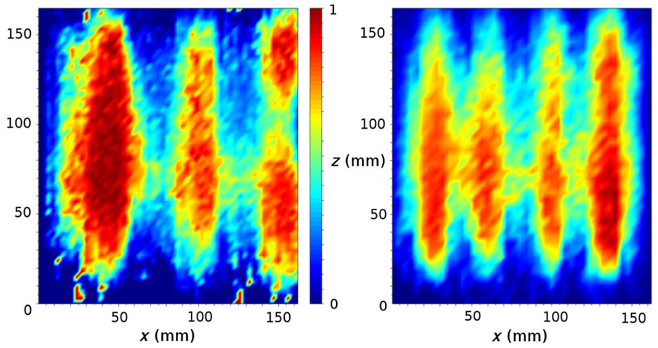

FIG. 6. Two-dimensional particle concentration fields. (Left) A system divided into six axial segments of width $\Delta L = 27$ mm, arranged in an alternating pattern of concave (pentagramal) and convex (pentagonal) segments, beginning at $x = 0$ with a concave geometry. (Right) A series of nine similar segments with $\Delta L = 18$ mm, beginning and ending with a concave geometry. In each image, red represents a region occupied entirely by h particles, while blue represents a pure region of l particles. For both systems, ($\phi_m^h = 0.5$) and $f = \frac{1}{3}$.

subdividing the experimental data into overlapping time windows and comparing the fields produced by each window, it is possible to determine an upper limit on the time scale for segregation by determining the approximate point at which the system reaches its steady state. Our data suggest that the segregative process is complete after no more than 1 h; however, it is highly possible that the true time scale is significantly shorter than this upper threshold. The determination of an accurate time scale for the geometrically induced segregation of bidisperse-by-density systems represents a valuable direction for future research.

The ability to induce axial banding in d systems, where such segregation is, under otherwise identical circumstances, absent can be explained through a loose analogy with the work of Zik *et al.* [2] in s systems, who showed that an axial modulation in the diameter of a drum could induce a local change in the angle of repose, θ. This spatial modulation would prompt (more mobile) larger particles to predominantly flow towards this region, thus further lowering θ, attracting still larger particles and so on until strong axial segregation is achieved. In d systems, however, as previously noted, the requisite difference in the angle of repose between species is seemingly absent, i.e., the diameter modulation exploited by Zik *et al.* [2] is unlikely to induce segregation—hence, the decision to instead implement a convex-concave geometry, which is known to impose axial variations in mean particle velocity [39]. Specifically, the peak velocities achieved in concave drum segments are considerably higher than in convex segments. In a given flow region, both species can be expected [57]—and indeed are observed—to possess equal mean velocities. In the present case of equally sized, identically shaped particles possessing equal velocities, the penetration length of a moving particle is directly proportional to its material density [58]. Thus, h particles from (faster-flowing)

concave sections are more likely to penetrate deep into adjacent convex regions, with l particles more likely to simply remain in their current segment. A simple pictorial representation of this proposed mechanism may be seen in Fig. 7. Direct evidence of this behavior can indeed be seen from our PEPT data, which shows h particles in the free-surface flow region of the system to exhibit greater mean axial displacement than l particles for equivalent downslope transits. Moreover, since h particles are more likely to displace l particles during their transit, l particles in convex regions are also more likely to be "pushed" to concave regions. As this process continues, the increased relative density of h particles in convex segments will make it progressively harder for l particles to enter these regions, and easier for them to enter concave regions, creating a positive feedback reminiscent of spinodal decomposition, and hence a strongly segregated final state. The proposed mechanism may also explain the reduced segregation observed at lower rotation rates, as the inherent reduction in particle velocity will render h particles in concave regions considerably less likely to penetrate far into neighboring sections. The reduced lateral transit of h particles at lower ω is also clearly reflected in our experimental data. The tendency of h particles to occupy convex—as opposed to concave—regions also makes sense in terms of energy minimization, as particles in these regions possess a lower average center of mass. Energy minimization has indeed recently been shown to be a key driving factor in the segregative behaviors of (vibrofluidized) granular beds [59].

It is valuable to note that the mechanisms underlying the axial segregation of bidisperse-by-density (d) systems are entirely distinct from all mechanisms currently proposed to explain the banding observed in s systems [2,40,60,61]—a further, notable refutation of the generally held assumption that our expectations of s systems can be generalized to equivalent d systems.

The variable system geometry allows both the positions and widths of l- and h-particle bands to be deliberately controlled. Thus, an arbitrary number of segregation patterns can be created (see, for example, Fig. 6). Moreover, the bands formed are seemingly free from the "coarsening" [62] observed in conventional systems: beds rotated for >24 h show no observable deviation from their initial segregated state. In other words, the bands formed are stable, permanent, and reproducible, as opposed to the transient, metastable bands observed in geometrically uniform beds [32,42,63], allowing a predictive knowledge of the particle distribution within our system—a potentially valuable ability for both future research and practical applications. The forced banding produced by the system's inhomogeneous geometry is found to persist for differing filling fractions ($\frac{1}{3} \leq f \leq \frac{2}{3}$), Froude numbers ($0.010 \leq \mathrm{Fr} \leq 0.052$) and relative particle concentration ($\frac{1}{3} \leq \phi_m^h \leq \frac{1}{2}$), although the variation of these parameters is found to affect the purity of the bands formed.

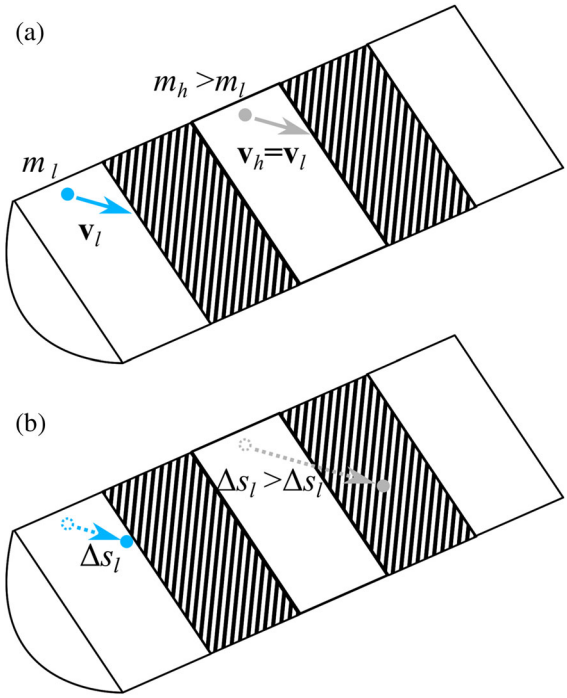

FIG. 7. Simple schematic diagram illustrating key concepts of our proposed mechanism for axial segregation. In the diagram, white segments represent concave regions, where particle velocities are relatively high compared to the adjacent convex regions (shaded). We depict a single pair of particles, one light glass particle (blue) and one heavy steel particle (gray). Both particles begin with equal velocity vectors $\mathbf{v}_l = \mathbf{v}_h$ and are placed at equivalent positions in two equivalent concave regions of the bed. We assume, for clarity and simplicity, the bed's makeup to be uniform other than for the asymmetric placement of the two particles depicted. As both particles have equivalent initial velocities but unequal masses, the h particle, which possesses higher momentum, will be able to penetrate more deeply into the slower-flowing (convex) neighboring section. Panels (a) and (b) show the system at two given points in time, t and $t + \Delta t$, respectively, where Δt is an arbitrary increment in time.

The strength of axial segregation is also found to exhibit a dependence of the length of the segments used, but not on the length of the drum as a whole. For example, two systems 72 and 144 mm long, each formed exclusively of alternating 18-mm segments, are observed to form equally clearly defined bands. Conversely, a 162-mm system comprising six 27-mm segments is found to display stronger segregation than a similar system composed of two 81-mm sections. Our data broadly suggest an approximately consistent segregation strength for relatively short segment lengths ($dx \lesssim 36$ mm) but a weakening of this segregation for longer segments, although further work is required to confirm and establish the functional form of this relation. In general, as the strength of axial segregation increases (decreases), the uniformity of the radial core diameter decreases (increases)—i.e., the strength of radial segregation is, as one may intuitively expect, inversely proportional to that of axial segregation.

Because of the multiple control parameters associated with rotating systems and the accordingly expansive parameter space to be explored, further research is required to fully establish the optimal conditions for segregation. For the purposes of this paper, it suffices to note that the phenomena discussed are not limited to a specific or restrictive parameter set.

The findings of this paper—particularly our discovery of a means through which axial segregation may be induced in bidisperse-by-density systems—carry potentially significant industrial applications. For instance, rotating-drum systems are often used in a variety of industrial processes in which heating of the granulate is required—examples include coating, drying, the induction of chemical reactions, and a variety of processes in the food sector. As discussed above, by inducing axial segregation, we also act to inhibit radial segregation [20]. Particles of both species are thus encouraged to explore the full radial extent of the system in a manner not possible in strongly radially segregated beds; the ability of particles of both species to access the full radial extent of the bed is easily confirmed by our PEPT data. As such, in our strongly axially segregated systems, the contact time between particles and the walls of the system (where heating will typically predominantly occur [64]) will me more even between dissimilar species, thus significantly aiding the uniformity of heating within the system.

IV. SUMMARY AND CONCLUSIONS

Using experimental data acquired using PEPT, we provide evidence of density-induced axial banding, achieved via the exploitation of nonuniform system geometries. Moreover, we have demonstrated that, using modified system geometries, it is possible to directly control the axial patterning exhibited by a system, producing a predetermined number of stable axial bands, with known positions and sizes. The mechanism underlying the observed segregative process is found to be entirely distinct from those which create banding in bidisperse-by-size (s) systems.

Our results in general emphasize that the behaviors of bidisperse-by-density systems cannot be predicted from, or understood using, our knowledge of s systems, underlining the need to further study the currently under-researched systems explored here.

Our observations carry potentially important applications both for a number of widely utilized industrial processes and for future research.

ACKNOWLEDGMENTS

The authors would like to thank Dr. Thomas Weinhart for the fruitful discussions, and the Dutch Technology Foundation STW for its financial support of STW-Vidi Project No. 13472, "Shaping Segregation: Advanced Modelling of Segregation and its Application to Industrial Processes", "Bridging the gap between granular systems and continuum theory." Furthermore, the authors would like to express their gratitude to the late Dr. Michael Hawkesworth, whose generous provision of funding from the Hawkesworth Scholarship has made the PEPT experiments possible.

[1] J. C. Williams, The segregation of powders and granular materials, Fuel Soc. J. **14**, 29 (1963).
[2] O. Zik, Dov Levine, S. G. Lipson, S. Shtrikman, and J. Stavans, Rotationally Induced Segregation of Granular Materials, Phys. Rev. Lett. **73**, 644 (1994).
[3] Anthony Rosato, Katherine J. Strandburg, Friedrich Prinz, and Robert H. Swendsen, Why the Brazil Nuts Are on Top: Size Segregation of Particulate Matter by Shaking, Phys. Rev. Lett. **58**, 1038 (1987).
[4] Tamás Börzsönyi and Ralf Stannarius, Granular materials composed of shape-anisotropic grains, Soft Matter **9**, 7401 (2013).
[5] Pik-Yin Lai, L.-C. Jia, and C. K. Chan, Friction Induced Segregation of a Granular Binary Mixture in a Rotating Drum, Phys. Rev. Lett. **79**, 4994 (1997).
[6] James W. Vallance and Stuart B. Savage, in *Proceedings of the IUTAM Symposium on Segregation in Granular Flows, Cape May, NJ, 2000*, edited by Anthony D. Rosato and Denis L. Blackmore, Solid Mechanics and Its Applications Vol. 81 (Springer, New York, 2000), p. 31.
[7] J. Duran, *Sands, Powders, and Grains* (Springer, New York, 2000).
[8] Guy Metcalfe and Mark Shattuck, Pattern formation during mixing and segregation of flowing granular materials, Physica (Amsterdam) **233A**, 709 (1996).
[9] Fernando J. Muzzio, Troy Shinbrot, and Benjamin J. Glasser, Powder technology in the pharmaceutical industry: The need to catch up fast, Powder Technol. **124**, 1 (2002).
[10] C. Zeilstra, M. A. Van Der Hoef, and J. A. M. Kuipers, Simulation of density segregation in vibrated beds, Phys. Rev. E **77**, 031309 (2008).
[11] Nusruth Mohabuth, Philip Hall, and Nicholas Miles, Investigating the use of vertical vibration to recover metal from electrical and electronic waste, Minerals engineering **20**, 926 (2007).
[12] Weihong Xing and Charles Hendriks, Decontamination of granular wastes by mining separation techniques, J. Cleaner Prod. **14**, 748 (2006).
[13] Xiao Yan Liu, E. Specht, and J. Mellmann, Experimental study of the lower and upper angles of repose of granular materials in rotating drums, Powder Technol. **154**, 125 (2005).
[14] Steven W. Meier, Richard M. Lueptow, and Julio M. Ottino, A dynamical systems approach to mixing and segregation of granular materials in tumblers, Adv. Phys. **56**, 757 (2007).
[15] G. Seiden and Peter J. Thomas, Complexity, segregation, and pattern formation in rotating-drum flows, Rev. Mod. Phys. **83**, 1323 (2011).

[16] F. Cantelaube and D. Bideau, Radial segregation in a 2D drum: An experimental analysis, Europhys. Lett. **30**, 133 (1995).
[17] D. V. Khakhar, J. J. McCarthy, and J. M. Ottino, Radial segregation of granular mixtures in rotating cylinders, Phys. Fluids **9**, 3600 (1997).
[18] Nitin Jain, Julio M. Ottino, and Richard M. Lueptow, Regimes of segregation and mixing in combined size and density granular systems: An experimental study, Granular Matter **7**, 69 (2005).
[19] S. Das Gupta, D. V. Khakhar, and S. K. Bhatia, Axial segregation of particles in a horizontal rotating cylinder, Chem. Eng. Sci. **46**, 1513 (1991).
[20] K. M. Hill, A. Caprihan, and J. Kakalios, Axial segregation of granular media rotated in a drum mixer: Pattern evolution, Phys. Rev. E **56**, 4386 (1997).
[21] K. M. Hill, A. Caprihan, and J. Kakalios, Bulk Segregation in Rotated Granular Material Measured by Magnetic Resonance Imaging, Phys. Rev. Lett. **78**, 50 (1997).
[22] I. Zuriguel, J. F. Boudet, Y. Amarouchene, and H. Kellay, Role of Fluctuation-Induced Interactions in the Axial Segregation of Granular Materials, Phys. Rev. Lett. **95**, 258002 (2005).
[23] Suman K. Hajra and D. V. Khakhar, Radial segregation of ternary granular mixtures in rotating cylinders, Granular Matter **13**, 475 (2011).
[24] M. Alonso, M. Satoh, and K. Miyanami, Optimum combination of size ratio, density ratio and concentration to minimize free surface segregation, Powder Technol. **68**, 145 (1991).
[25] G. G. Pereira, N. Tran, and P. W. Cleary, Segregation of combined size and density varying binary granular mixtures in a slowly rotating tumbler, Granular Matter **16**, 711 (2014).
[26] Lori Sanfratello and Eiichi Fukushima, Experimental studies of density segregation in the 3D rotating cylinder and the absence of banding, Granular Matter **11**, 73 (2009).
[27] G. G. Pereira, M. D. Sinnott, P. W. Cleary, Kurt Liffman, Guy Metcalfe, and Ilija D. Šutalo, Insights from simulations into mechanisms for density segregation of granular mixtures in rotating cylinders, Granular Matter **13**, 53 (2011).
[28] Shakil Ahmed, Sam E. John, Ilija D. Šutalo, Guy Metcalfe, and Kurt Liffman, Experimental study of density segregation at end walls in a horizontal rotating cylinder saturated with fluid: Friction to lubrication transition, Granular Matter **14**, 319 (2012).
[29] M. M. H. D. Arntz, H. H. Beeftink, den W. K. Otter, W. J. Briels, and R. M. Boom, Segregation of granular particles by mass, radius, and density in a horizontal rotating drum, AIChE J. **60**, 50 (2014).
[30] D. R. Tunuguntla, O. Bokhove, and A. R. Thornton, A mixture theory for size and density segregation in shallow granular free-surface flows, J. Fluid Mech. **749**, 99 (2014).
[31] D. R. Tunuguntla and A. R. Thornton, in Proceedings of the 8th International Conference on Micromechanics of Granular Media, Montpellier, France, 2017 [*EPJ Web Conf.* 140, 03079 (2017)].
[32] K. M. Hill and J. Kakalios, Reversible axial segregation of binary mixtures of granular materials, Phys. Rev. E **49**, R3610 (1994).
[33] Steven W. Meier, Diego A. Melani Barreiro, Julio M. Ottino, and Richard M. Lueptow, Coarsening of granular segregation patterns in quasi-two-dimensional tumblers, Nat. Phys. **4**, 244 (2008).
[34] Throughout this paper, the authors draw distinction between the end-wall-induced effects observed by Pereira and coworkers [25,27] and the phenomenon which we term axial banding. While both the former and the latter certainly represent forms of axial segregation, we reserve the term "banding" for the case in which repeated axial sections or bands of high single-species concentration are observed throughout the axial extent of a system.
[35] K. M. Hill, Nitin Jain, and J. M. Ottino, Modes of granular segregation in a noncircular rotating cylinder, Phys. Rev. E **64**, 011302 (2001).
[36] Steven W. Meier, Stephen E. Cisar, Richard M. Lueptow, and Julio M. Ottino, Capturing patterns and symmetries in chaotic granular flow, Phys. Rev. E **74**, 031310 (2006).
[37] Ivan C. Christov, Julio M. Ottino, and Richard M. Lueptow, Chaotic mixing via streamline jumping in quasi-two-dimensional tumbled granular flows, Chaos **20**, 023102 (2010).
[38] D. V. N. Prasad and D. V. Khakhar, Mixing of granular material in rotating cylinders with noncircular cross-sections, Phys. Fluids **22**, 103302 (2010).
[39] S. González, C. R. K. Windows-Yule, S. Luding, D. J. Parker, and A. R. Thornton, Forced axial segregation in axially inhomogeneous rotating systems, Phys. Rev. E **92**, 022202 (2015).
[40] C. R. K. Windows-Yule, B. J. Scheper, A. J. van der Horn, N. Hainsworth, J. Saunders, D. J. Parker, and A. R. Thornton, Understanding and exploiting competing segregation mechanisms in horizontally rotated granular media, New J. Phys. **18**, 023013 (2016).
[41] M. M. H. D. Arntz, W. K. Den Otter, W. J. Briels, P. J. T. Bussmann, H. H. Beeftink, and R. M. Boom, Granular mixing and segregation in a horizontal rotating drum: A simulation study on the impact of rotational speed and fill level, AIChE J. **54**, 3133 (2008).
[42] K. M. Hill and J. Kakalios, Reversible axial segregation of rotating granular media, Phys. Rev. E **52**, 4393 (1995).
[43] G. Juarez, J. M. Ottino, and R. M. Lueptow, Axial band scaling for bidisperse mixtures in granular tumblers, Phys. Rev. E **78**, 031306 (2008).
[44] D. J. Parker, R. N. Forster, P. Fowles, and P. S. Takhar, Positron emission particle tracking using the new Birmingham positron camera, Nucl. Instrum. Methods Phys. Res., Sect. A **477**, 540 (2002).
[45] R. D. Wildman, J. M. Huntley, J.-P. Hansen, D. J. Parker, and D. A. Allen, Single-particle motion in three-dimensional vibrofluidized granular beds, Phys. Rev. E **62**, 3826 (2000).
[46] D. J. Parker, A. E. Dijkstra, T. W. Martin, and J. P. K. Seville, Positron emission particle tracking studies of spherical particle motion in rotating drums, Chem. Eng. Sci. **52**, 2011 (1997).
[47] Y. L. Ding, R. Forster, J. P. K. Seville, and D. J. Parker, Segregation of granular flow in the transverse plane of a

rolling mode rotating drum, Int. J. Multiphase Flow **28**, 635 (2002).

[48] R. Y. Yang, R. P. Zou, and A. B. Yu, Microdynamic analysis of particle flow in a horizontal rotating drum, Powder Technol. **130**, 138 (2003).

[49] A. Ingram, J. P. K. Seville, D. J. Parker, X. Fan, and R. G. Forster, Axial and radial dispersion in rolling mode rotating drums, Powder Technol. **158**, 76 (2005).

[50] R. Y. Yang, A. B. Yu, Luke McElroy, and J. Bao, Numerical simulation of particle dynamics in different flow regimes in a rotating drum, Powder Technol. **188**, 170 (2008).

[51] C. T. Jayasundara, R. Y. Yang, B. Y. Guo, A. B. Yu, I. Govender, A. Mainza, A. Van der Westhuizen, and J. Rubenstein, CFD-DEM modelling of particle flow in IsaMills—Comparison between simulations and PEPT measurements, Minerals engineering **24**, 181 (2011).

[52] D. J. Parker, C. J. Broadbent, P. Fowles, M. R. Hawkesworth, and P. McNeil, Positron emission particle tracking—A technique for studying flow within engineering equipment, Nucl. Instrum. Methods Phys. Res., Sect. A **326**, 592 (1993).

[53] C. R. K. Windows-Yule, T. Weinhart, D. J. Parker, and A. R. Thornton, Influence of thermal convection on density segregation in a vibrated binary granular system, Phys. Rev. E **89**, 022202 (2014).

[54] C. R. K. Windows-Yule, T. Weinhart, D. J. Parker, and A. R. Thornton, Effects of Packing Density on the Segregative Behaviors of Granular Systems, Phys. Rev. Lett. **112**, 098001 (2014).

[55] R. D. Wildman and D. J. Parker, Coexistence of Two Granular Temperatures in Binary Vibrofluidized Beds, Phys. Rev. Lett. **88**, 064301 (2002).

[56] Masami Nakagawa, Stephen A. Altobelli, Arvind Caprihan, and Eiichi Fukushima, NMRI study: Asial migration of radially segregated core of granular mixtures in a horizontal rotating cylinder, Chem. Eng. Sci. **52**, 4423 (1997).

[57] J. M. Ottino and D. V. Khakhar, Scaling of granular flow processes: From surface flows to design rules, AIChE J. **48**, 2157 (2002).

[58] D. A. Huerta and J. C. Ruiz-Suárez, Vibration-Induced Granular Segregation: A Phenomenon Driven by Three Mechanisms, Phys. Rev. Lett. **92**, 114301 (2004).

[59] C. R. K. Windows-Yule, B. J. Scheper, W. K. den Otter, D. J. Parker, and A. R. Thornton, Modifying self-assembly and species separation in three-dimensional systems of shape-anisotropic particles, Phys. Rev. E **93**, 020901 (2016).

[60] Yi Fan and K. M. Hill, Phase Transitions in Shear-Induced Segregation of Granular Materials, Phys. Rev. Lett. **106**, 218301 (2011).

[61] Yi Fan and K. M. Hill, Theory for shear-induced segregation of dense granular mixtures, New J. Phys. **13**, 095009 (2011).

[62] Tilo Finger, Andreas Voigt, Jörg Stadler, Heiko G. Niessen, Lama Naji, and Ralf Stannarius, Coarsening of axial segregation patterns of slurries in a horizontally rotating drum, Phys. Rev. E **74**, 031312 (2006).

[63] Nicolas Taberlet, Wolfgang Losert, and Patrick Richard, Understanding the dynamics of segregation bands of simulated granular material in a rotating drum, Europhys. Lett. **68**, 522 (2004).

[64] Qiang Xie, Zuobing Chen, Qinfu Hou, A. B. Yu, and Runyu Yang, DEM investigation of heat transfer in a drum mixer with lifters, Powder Technol. **314**, 175 (2017).